varying from 0.2 to 0.5 μ (0.4 μ average) in length and 60 to 120 Å in diameter at the center. The end portions had large irregular projections similar to some examples illustrated by Huxley. The filaments, however, were not spindle-shaped, and the large irregularities were clearly discernible at low magnification (Fig. 2*b*). This is a consistently reproducible preparation, and it appears that the particular *p*H of the medium is a factor determining the size and characteristics of these filaments.

BENJAMIN KAMINER
ALLEN L. BELL
Institute for Muscle Research, Marine Biological Laboratory, Woods Hole, Massachusetts, and *Department of Anatomy, State University of New York, Syracuse*

References and Notes

1. H. E. Huxley, *J. Mol. Biol.* **7**, 28 (1963).
2. A. Szent-Györgyi, *Chemistry of Muscular Contraction* (Academic Press, New York, ed. 2, 1951).
3. H. Portzell, G. Schramm, H. H. Weber, *Z. Naturforsch.* **58**, 61 (1950).
4. Supported by NIH grant GM-10383 and NSF grant G5836.

8 October 1965

Liquid Water in Frozen Tissue: Study by Nuclear Magnetic Resonance

Abstract. *Nuclear magnetic resonance (NMR) spectroscopy was used to examine the behavior and extent of liquid water in postrigor-frozen tissue of cod at temperatures below 0°C. A liquid-water phase persists in the tissue down to about −70°C; the extent of the phase decreases rapidly between 0° and −10°C and slowly at lower temperatures. That the NMR absorption peak of the liquid water increases in width, with decreasing temperature, suggests loss of mobility or structuring of the phase. A technique for introducing geometrically uniform cores of muscle into the probe of the high-resolution spectrometer permits quantitative determinations of liquid water.*

Information on the behavior of water in frozen tissue at temperatures below 0°C relates to understanding of the mechanisms of protein denaturation and tissue degradation during frozen storage, and may throw light on the complex role of water in the living cell. We now report results of nuclear magnetic resonance (NMR) spectroscopic examination (*1*) of postrigor-frozen muscle of cod (*Gadus morhua*).

Quantitative determinations of liquid water were made on geometrically uniform cores of tissue cut from fillets of dorsal muscle of fresh cod with a modified 5-mm Varian A-60 sample tube. The tube was modified (Fig. 1) by cutting-off the sealed end and by grinding a scalloped cutting edge on that end. When screwed into the fish fillet, the tube cut a core of tissue that remained within the tube; the lower end of the tube was then closed with a 5-mm plug of window putty. The tube, with core sample (at least 4 cm long), was inserted in the Varian A-60 probe to a depth of 3 mm above the temperature sensor, and the sample was rotated at 20 to 40 rev sec^{-1}. Spectra consisted of a single, broad, symmetrical peak whose position downfield of tetramethylsilane coincided with that of distilled water at the same temperature. If air bubbles or other gross inhomogeneities were introduced with the sample, spinning side bands appeared and peak shape was distorted. The core-cutting sample tube reduces "filling factor" variability, which hinders quantitative NMR measurements on nonliquid materials (*2*). Liquid-water content of tissue was obtained from NMR absorption-peak area by comparing the tissue-water peak area with the area of the water peak of a 23.3 percent NaCl (eutectic) solution at the same temperature. Weight-percentage of tissue water was calculated as follows:

$$\text{Liquid water (percent)} = (A_{tissue}/A_{eutectic})\ 0.766\ (\rho_{eutectic}/\rho_{tissue})$$

where A is the peak area (of tissue or eutectic solution), 0.766 is the weight in grams of liquid water per gram of eutectic solution, and ρ is the density (of tissue or eutectic solution) at 20°C. The validity of the calculation is shown by Fig. 2, which serves as a calibration chart and which plots known water contents of saline solutions of different concentrations (0.9, 3.0, 8.0, 16, and 23.3 percent NaCl) against the above function of peak-area ratio at temperatures between 38° and −21°C. Between 0° and −21.1°C the noneutectic solutions deposited varying amounts of pure ice. Their liquid-water contents depended on temperature and initial concentration and were computed from the NaCl-ice phase diagram; the points below 20 percent water in Fig. 2 represent such ice-salt solution mix-

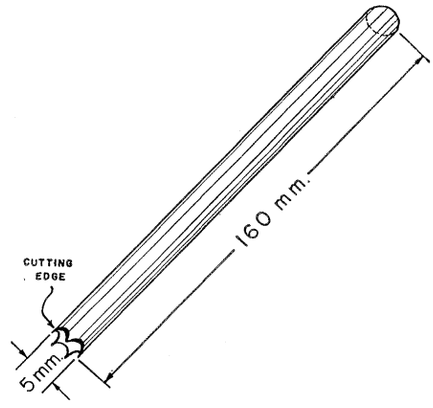

Fig. 1. Core-cutting sampling tube for NMR spectroscopy.

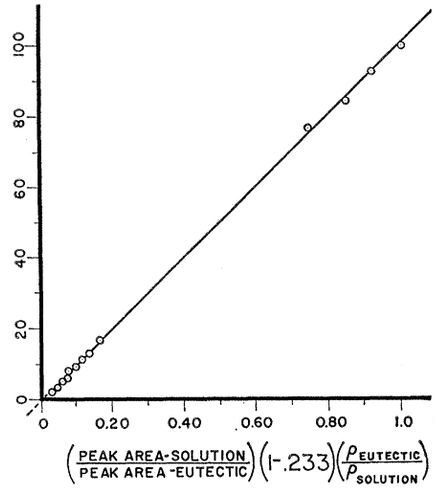

Fig. 2. Calibration curve: NMR peak-area ratio as a function of percentage by weight of liquid water (ordinate).

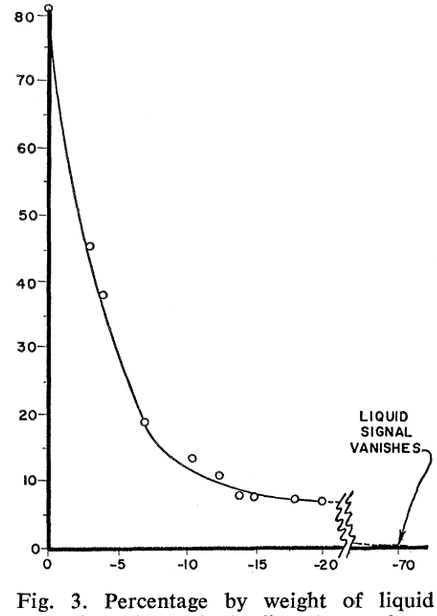

Fig. 3. Percentage by weight of liquid water in cod muscle (ordinate) as a function of temperature (Celsius, abscissa).

tures. A 45-degree straight line drawn through the origin connects all these calibration points; this suggests absence of radio-frequency saturation, good field uniformity, and a constant line-shape function, all factors that tend to make peak area directly proportional to the number of resonating protons per unit volume of sample (*2, 3*).

The variation in the liquid-water content of cod fillet with temperature is shown in Fig. 3; the data, for the same sample of tissue, indicate that rapid decrease in content between 0° and −10°C is followed by a slow decrease at lower temperatures. Quantitative measurements were made down to −20°C. Qualitative measurements on a wide-band spectrometer, at temperatures below −20°C, show that the liquid-water spectrum exists at −68°C and disappears at about −70°C (*4, 5*).

Figure 4 shows the variation in absorption-peak width with temperature. Peak width, measured at 0.6 of peak maximum, increases with decreasing temperature, suggesting a loss of mobility, or increase in structuring of water molecules, with decrease in extent of the liquid phase and in temperature. Water-peak widening has been reported (*6*) for water in clays at temperatures below 0°C, as well as an increase in water-peak width as the water content of various natural materials, particularly starch, decreases (*7*).

Peak width at temperatures between 20° and 0°C is about 10 cy/sec, compared with about 2 cy/sec for pure distilled water and 7 cy/sec for the "Homo-adjust" standard (a solution of paramagnetic salts) used with the A-60 machine. Below 0°C the peak widens rapidly, reaching 140 cy/sec at −19°C. Broadening of NMR water signals (or decrease in transverse relaxation time) in the presence of DNA, human cells, starches, and other materials (*8, 9*) has been ascribed to loss of mobility and structuring of the liquid water by processes such as H-bonding, adsorption, gelation, hydration, and others. The broadened tissue peak is still much narrower than a pure-ice peak; comparison of the two on a wide-band spectrometer (*5*) showed the peak width of pure ice to be 70 times greater than that of the liquid water of fish muscle at −16°C.

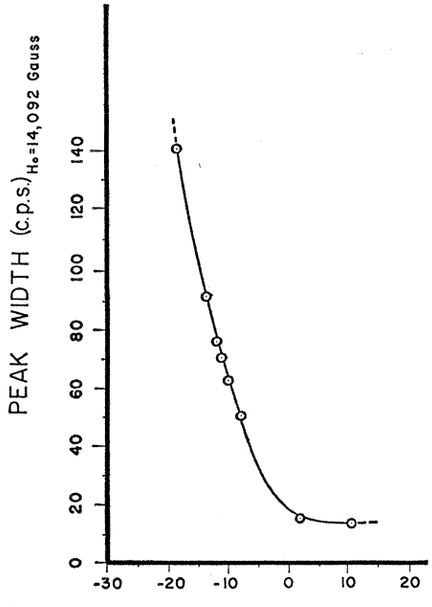

Fig. 4. Peak width (NMR spectroscopy) as a function of temperature (Celsius, abscissa).

The rapid freezing rate followed by the slow freezing (Fig. 3) may be interpretable in terms of freezing of "free" and "bound" water phases, the concept of "bound" water having something of a tradition in discussions of cellular water (*9, 10*). Figure 4, however, showing no sharp slope changes below 0°C, indicative of a disappearance of phase, suggests that the change in binding is gradual and probably involves a spectrum of binding energies.

Most estimates of the extent of liquid phase in frozen tissue, based on calorimetric, histological, dilatometric, and thermal-conductivity observations, agree that most of the liquid phase is solidified at or above −20°C. Estimates of the temperature of complete solidification of animal tissue vary from −20°C to −65°C (*10*). Riedel (*11*) reports that cod muscle freezes completely below −65°C.

M. V. Sussman
L. Chin
Department of Chemical Engineering, Tufts University, Medford, Massachusetts

References and Notes

1. With a Varian A-60 high-resolution spectrometer fitted with a model V-6057 controlled-temperature probe, which was adjusted for optimum field homogeneity and "ringing" before each run.
2. T. M. Shaw and R. H. Elsken, *J. Appl. Phys.* **26**, 313 (1955); *Anal. Chem.* **27**, 1983 (1955).
3. J. A. Pople, W. G. Schneider, H. J. Bernstein, *High Resolution NMR Spectroscopy* (McGraw-Hill, New York, 1959).
4. The water content of muscle of fresh cod at probe temperature (38°C), determined by NMR measurement on 51 samples taken from five fish, is 81 ± 2 percent. Precision of an individual peak-area measurement is estimated to be within 1.5 percent.
5. Wide-line spectra were run for us by Rainer Mattes in E. Rochow's laboratory at Harvard University; we thank both.
6. T. H. J. Wu, *Geophys. Res.* **69**, 1083 (1964).
7. T. M. Shaw and R. H. Elsken, *J. Chem. Phys.* **21**, 565 (1953).
8. B. Jacobsohn, W. A. Anderson, J. T. Arnold, *Nature* **173**, 772 (1954); O. Hechter, T. Wittstruck, N. McNiven, G. Lester, *Proc. Nat. Acad. Sci. U.S.* **46**, 783 (1960); E. Odelblad, *Ann. N.Y. Acad. Sci.* **83**, 189 (1959).
9. C. B. Bratton, A. L. Hopkins, J. W. Weinberg, *Science* **147**, 738 (1965).
10. R. M. Love, in *Cryobiology*, H. T. Meryman, Ed. (in press), chap. 7.
11. L. Riedel, *Kaltetechnik* **8**, 374 (1956).
12. This work was supported by the U.S. Bureau of Commercial Fisheries Technological Laboratory, Gloucester, Mass.

12 November 1965

Manganese Nodules: Their Evolution

Abstract. *That manganese nodules and adjacent deep-sea sediments are accumulating manganese at almost the same rate has been established by thorium-230 dating of both sediments and nodules of known manganese content. The rate of manganese deposition is nearly constant over the world oceans. A relatively simple model of nodule evolution explains the distribution of manganese nodules between sediment column and sediment-water interface; the model appears to apply to other trace elements such as copper, nickel, and cobalt.*

Since Murray and Renard (*1*) first reported the discovery of manganese nodules by the *Challenger* expedition (1873–76), many workers have speculated regarding the origin of these ferromanganese oxide concretions. Kuenen (*2*) reviewed the evidence that the nodules grow by slow accumulation of authigenic manganese. More recently Bonatti and Nayudu (*3*) discussed indications that manganese nodules are formed by rapid accumulation of manganese coming from submarine volcanic exhalates. The composition, mineralogy, occurrence, and theories regarding the evolution of nodules were recently discussed extensively by Mero (*4*) and Menard (*5*).

We propose the following simple model, based on our findings, for the evolution of manganese nodules. The relatively constant rates at which manganese accumulates in deep-sea sediments (Table 1) indicate that there is a rather uniform "rain" of manganese over the entire ocean floor. Whereas most of this manganese is incorporated into deep-sea sediments, hard bodies such as sharks' teeth and volcanic fragments lying on the sediment surface